Cosmic rays

Note: we have entered the era of multi messenger astronomy:
Parallel observation of

- UHECR
- Photons of different energies (radio, light, x-ray, gamma-rays)
- High energy neutrinos
- Gravitational waves

All of above observation techniques would deserve an individual lecture. Here we will only deal with UHECRs and gamma rays. Next semester: gravitational waves!

2. Observation of Ultra-high energy (UHE) cosmic rays and gamma astronomy

Detection of cosmic rays depends on energy range and on particle type. In general: satellite experiments, balloon experiments, detection of particle showers.
For UHE cosmic rays: Flux is very low (for 10^{15} eV ~ 1 event per m^2 per year)
→ Need large detector area
→ Satellite experiments not suitable

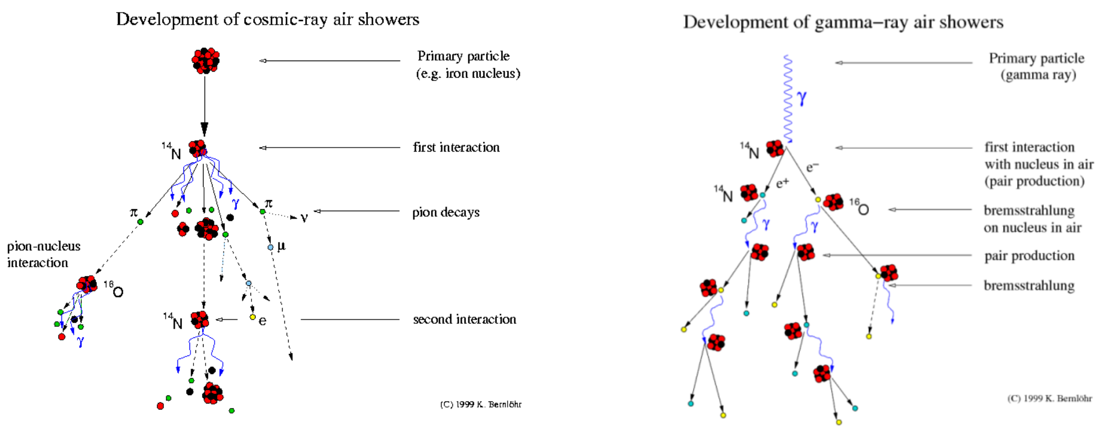

Creation of particle showers in the atmosphere induced by nucleus (left) and gamma (right). While a nucleus in average undergoes more than one interaction within the atmosphere leading to pions, gamma rays mostly leads to Bremsstrahlung und pair production.

<u>Detection of particle showers:</u>
If Ultra High Energy (UHE) cosmic rays or gamma rays hit the atmosphere, they create a particle shower. First interaction is at height ~10km.
The development of the air shower depends on the type of particle impinging onto the atmosphere.

Highest energetic particles can be detected by:
secondary particles on earth surface: muons, pinons, protons….

fluorescence light created by excited nitrogen in atmosphere
Radio emission due to net drift of charged particles in shower due to interaction with geomagnetic field

→ Displacement of positive and negative charges
→ Change of particle density

→EM pulse!

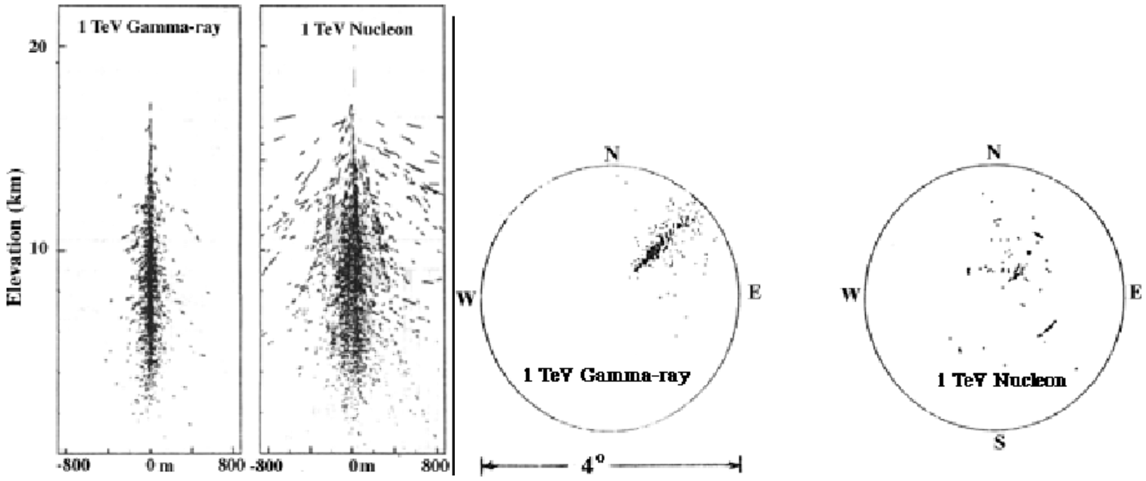

The particles in an air shower (left) are much more widely distributed for proton than for gamma-ray showers. This is reflected in the distribution of photons in the detector (right). Figs. Taken from [http://www.gae.ucm.es/~emma/docs/tesina/node17.html].

The Pierre Auger Observatory:
1600 surface water **Čerenkov detectors** on surface of ~3000 km^2 located in Argentina.
Water Čerenkov detectors consist of 12 ton ultra clean water tanks viewed by three PMTs from the top.
Additionally four **fluorescence telescopes** view the active volume/area.
Pierre Auger upgrade 2019/2020: **Radio measurements** at 30-80MHz!
Complementary to scintillators at high zenith angles
Telescope Array (Utah, USA) follows very similar concept (3 FDs, 507 SDs).

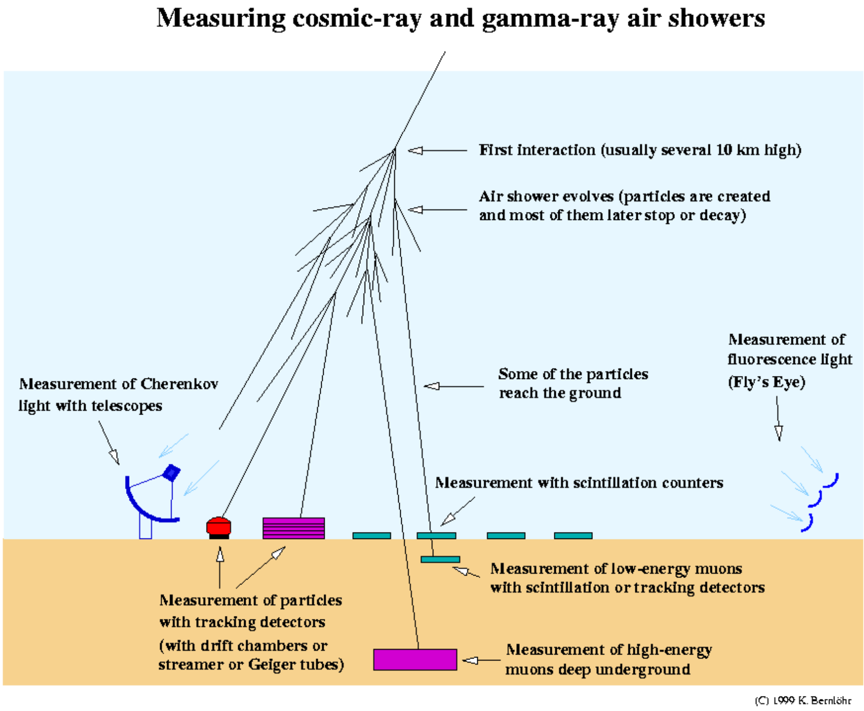

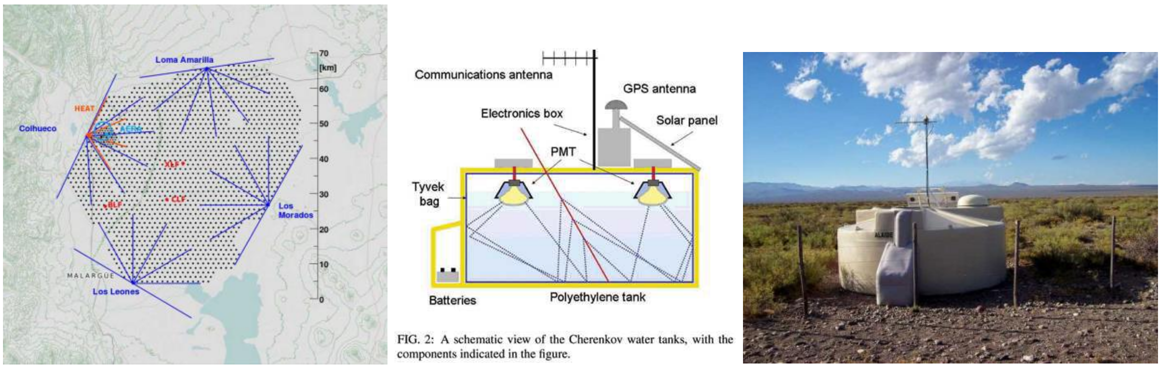

Left: map of the Pierre Auger observatory. Each black dot corresponds to one surface detector (SD). Four fluorescence detectors at the edge if the observatory view the area above. Center: Drawing of a SD. Right Picture af an SD.

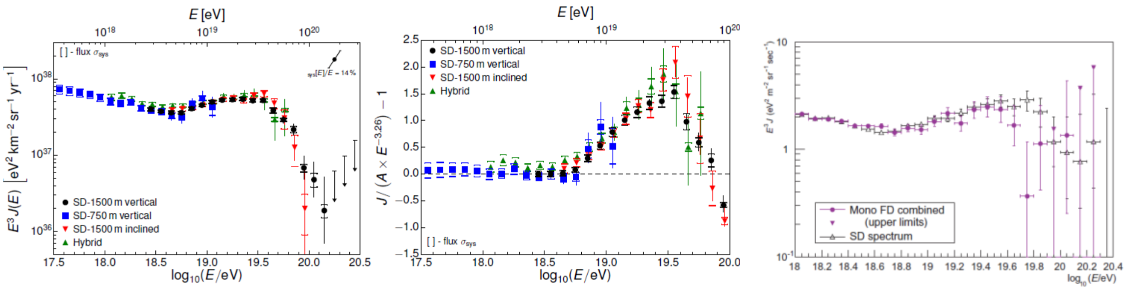

Left: energy spectra derived from surface detectors and hybrid data recorded at the Pierre Auger Observatory. The error bars represent statistical uncertainties. The upper limits correspond to the 84% C.L. Center: fractional difference between the Auger spectra and a reference spectrum with an index of 3.26. Taken from [arXiv: 1509.03732]. Right: Spectrum recorded with the Telescope array Taken from [Astropart. Phys. 48 (2013)16]

Observation of cosmic rays with energies up to $10^{20.2}$ eV.

A cutoff is clearly visible in the spectrum at ~10^{20}eV

→Observation of GZK cutoff?
→Observation of energy cutoff for acceleration mechanism?
Non-conclusive: mixture of both?

<u>Composition of UHE cosmic ray:</u>
The depth at which the shower reaches its maximum X_{max} is different for nuclei with different mass (dE/dx → Bethe Bloch).
Obtaining X_{max} distributions for different energies from measurement of fluorescent detectors, information can be obtained about the effective mass of the cosmic ray nuclei.

At highest energies: Composition of cosmic rays tends towards heavier elements!
→ Hint towards upper energy for acceleration mechanism?
→Higher mass nuclei exceed GZK limit for protons, i.e. no contradiction!

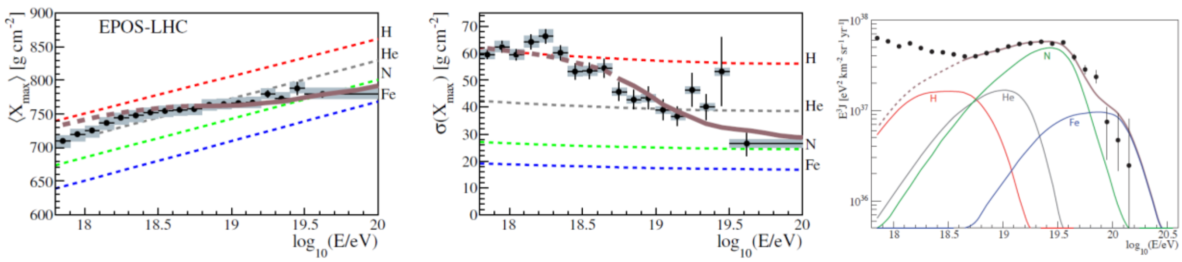

Left and center [taken from EPJ Web of Conferences 209, 01002 (2019)]: Average and standard deviation of the X_{max} distribution, compared to those predicted for pure H (red dashed lines), He (grey), N (green) and Fe (blue). Also shown with brown lines are the predictions from the model with mixed composition illustrated in the right panel. Right: Energy spectrum compared to best-fit parameters for a specific propagation model along with data points from PA (taken from [arxiv:1612.08188])

<u>Angular distribution of UHE events:</u>
For $E \sim 10^{20}$eV: Expect distribution information roughly maintained if within ~ Mpc (some Star Burst Galaxies and AGNs).
→ Search for correlation of $\mathrm{E} > 5.3 \cdot 10^{19} eV$ (Larmor radius $r(55EeV, 10\mu G) \sim 5\ Mpc$) events with location of Active Galactic Nuclei?
Originally announced by Pierra Auger: *Science* **318**, 938 (2007)
Evidence has since disappeared

Charged particles are deflected by intergalactic magnetic fields
→ Expect isotropic distribution for cosmic rays with E<10^{19}eV

Liouville's theorem
→ CR distribution must be anisotropic outside galaxy for an anisotropy to be observed at Earth

→ Anisotropy cannot arise through deflections of an originally isotropic flux by a magnetic field.

PA observatory observes large scale anisotropy above $8{\cdot}10^{18}$ eV at 5.6 σ! Ongoing discussions for explanation…

Distribution seems to follow large scale structure fluctuations
Observation of correlation with Star Burst galaxies(SBG) & AGNs:
Test: Calculate how much better model containing anisotropic source explains observations than completely isotropic model

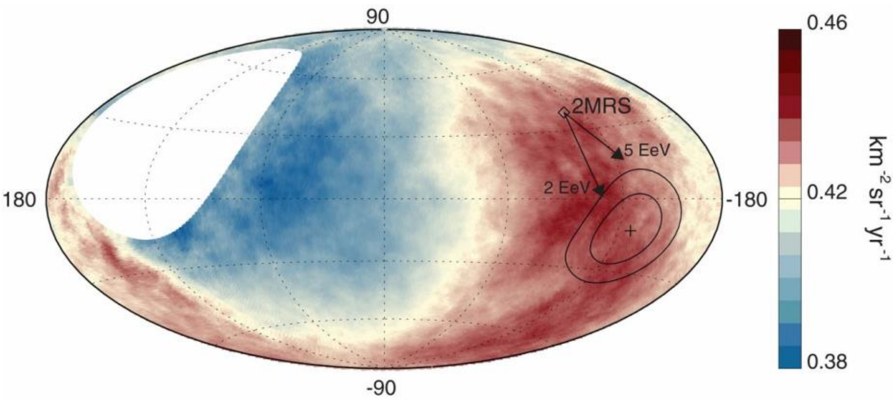

Sky map in galactic coordinates showing the cosmic-ray flux for $E \geq 8$ EeV smoothed with a 45° top-hat function. The galactic center is at the origin. The cross indicates the measured dipole direction; the contours denote the 68% and 95% confidence level regions. The dipole in the 2MRS galaxy distribution is indicated. Arrows show the deflections expected for a particular model of the galactic magnetic field (8) on particles with E/Z = 5 or 2 EeV. Taken from [A. Aab, Science 357, 1266 (2017)]

Used map of known sources (AGNs + SBGs)+ model for propagation to predict UHECR source distribution.
→ Test different models against isotropic distribution
→ **4.0σ for correlation with SBGs!**
→ **2.7σ for correlation with γAGNs**
Caution in interpretation: propagation model has uncertainties due to propagation effects!

THE ASTROPHYSICAL JOURNAL LETTERS, 853:L29 (10pp), 2018 February 1 :

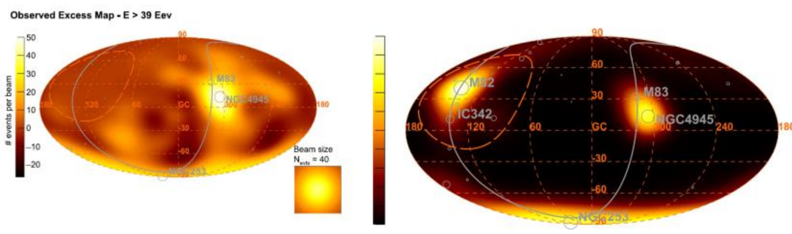

Observed excess map (left) and modelled excess map for UHECR with E>39MeV. Note that the area within the dashed line is outside of the field of view of the PA observatory!

Gamma Ray Astronomy:

Wherever high energetic processes are leading to acceleration of charged particles to extreme energies:

→Expect gamma rays from synchrotron radiation, inverse Compton Effect and via π^0 production! Difficult to disentangle between proton driven and inverse Compton Scattering spectra!

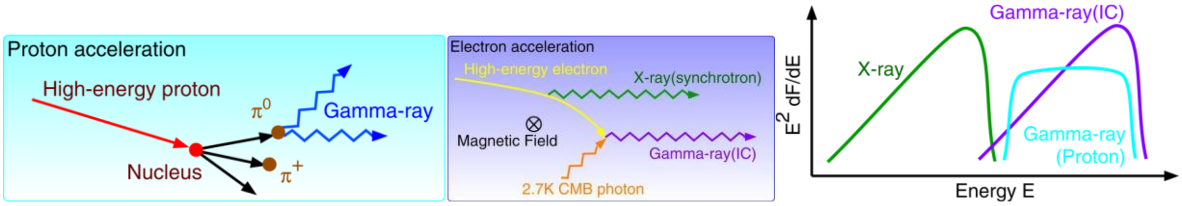

Possible production mechanisms for high energy gamma rays. Left: Proton acceleration can lead to pion production. Gammas emitted during the decay of π^0 are boosted. Center: A high energetic electron in a magnetic field can lead to synchrotron radiation or undergo inverse Compton scattering. Right: Expected shape of energy spectra for the three production mechanisms.

Gammas keep directional information → Identification of sources possible.

Possible sources:

Supernova remnants (Crab nebula), Binaries: White dwarf, red giant (V407 Cygni) , Pulsars (PSR J0101-6422), AGNs (Centaurus A), Blazars (PKS 0537-286)

Gamma Ray Bursts:

First observed in the 1960s by satellite mission designed to detect pulses from nuclear power tests.

Non terrestrial, i.e. cosmic origin of GRBs was concluded in 1973.

BATSE satellite measured direction of bursts

→ isotropic distribution

→ not galactic

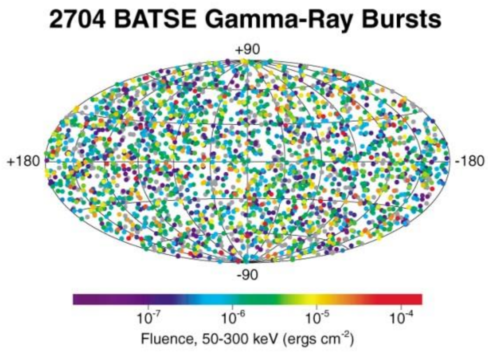

Locations of 2704 gamma-ray bursts detected by the BATSE instrument during nine years of observations. Statistical tests confirm that the bursts are isotropically distributed on the sky - no significant quadrupole moment or dipole moment is found. Taken from [heasarc.gsfc.nasa.gov]

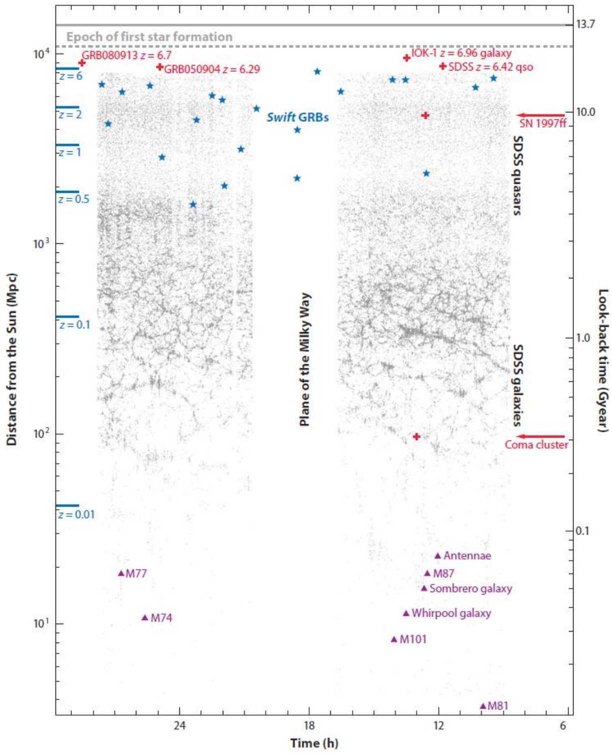

A 360◦ vista showing the entire sky, with visible structures stretching back in distance, time, and redshift. The most distant light we observe comes from the radiation leftover from the Big Bang: the CMB. As we descend the chart, we find the most distant objects known, followed by a web of Sloan Digital Sky Survey (SDSS) quasars and galaxies. Closer to home, we start to see a collection of familiar "near" galaxies (purple triangles). Also marked are all Swift GRBs with known distances (blue stars); SN 1997ff, the most distant type Ia supernova at z = 1.7; and the archetypal large galaxy cluster, the Coma cluster. The redshift distances of most distant GRBs are comparable to the most distant galaxies and quasars. Taken from [Annu. Rev. Astron. Astrophys. 47(2009.)567].

Beppo SAX satellite (1996-2002) could measure afterglows in very distant faint galaxies
→ cosmological distances
→ extremely powerful phenomena
Energy release in terms of gamma photons ~ $10^{43-47}J$ (up to 10^{59}photons per second during peak)!
Swift satellite: high-quality observations of hundreds of bursts, and facilitating a wide range of follow-up observations within seconds of each event.
Origin as of yet unclear: Probably shock front from merger of super dense objects: neutron stars, black holes…, jets from type SNII, Progenit
or: massive LBV/ Wolf-Rayet stars?
→example η-Carinae

Observation of astrophysical gamma rays:

Atmosphere prohibits direct detection of gammas: Absorption in atmosphere!

→ Two possibilities:

- Balloons, satellites
- Ground based: observation of showers

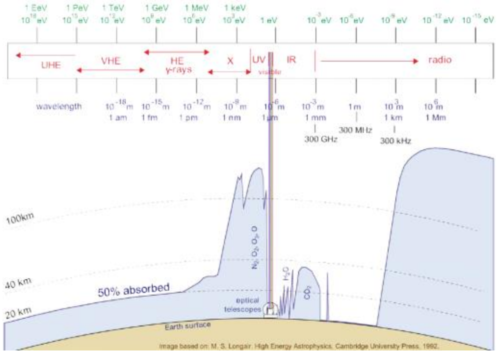

Transparency of earth atmosphere of radiation as function of frequency. The blue line represents the height at which 50% of the radiation of the given frequency is absorbed by the atmosphere. The atmosphere is transparent to visible light and radio frequencies, but not to gamma rays.

Satellite experiment: FERMI

International mission to perform gamma-tray astronomy with additional x-ray monitor for Gamma Ray Bursts (GRBs). FERMI was launched June 2008 and is taking data since Aug. 2008. Strategy: Survey 20% of sky at any time, entire sky every three hours (2 orbits)

FERMI-GBM (Gamma Burst Monitor):

12 (NaI) scintillators, each 12.7 cm in diameter by 1.27 cm thick, sensitive in the lower end of the energy range, from a few keV to about 1 MeV and provide burst triggers and locations

2 cylindrical BGO scintillators, each 12.7 cm in diameter and 12.7 cm in height.

cover the energy range ~150 keV to ~30 MeV, providing a good overlap with the NaI at the lower end and with the LAT at the high end.

FERMI-LAT (Large Area Telescope):

- Anti-coincidence detector: Detect background
  Plastic anticoincidence scintillator around outside made of 89 individual sections
  → distinguish charged particles from direction of incident gamma ray, ignore others
- Tracker: Direction
  18 tungsten converter layers + 16 dual silicon tracker
- Calorimeter: Energy
  96 long, narrow CsI scintillators in 8 layers, alternating orientation
  → Determination of location and spread of the deposited energy.

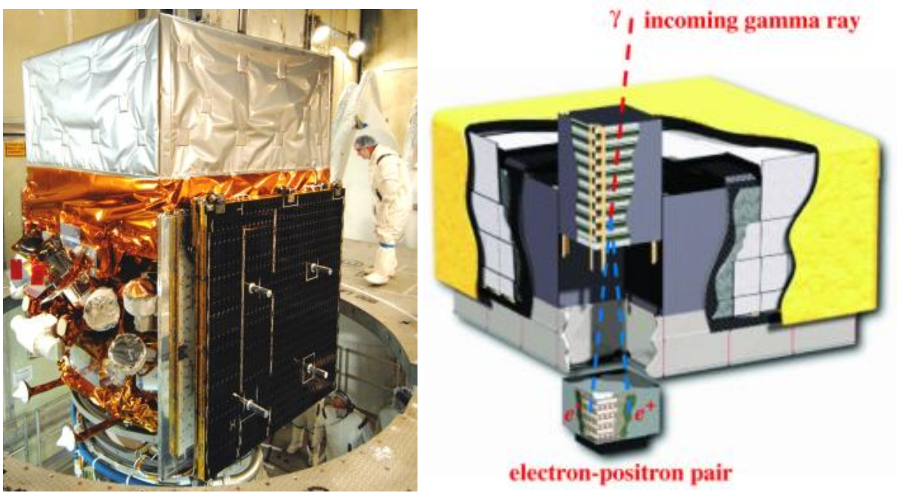

Left: The Fermi spacecraft shortly before launch. The solar panels are folded at the sides. The GBM detector modules and the telemetry antennas can be seen on the left side. Right: The 18 tungsten converter layers and 16 dual silicon tracker planes are stacked in 16 modular "towers" (37 cm square and 66 cm tall). Each of the 16 calorimeter modules consists of 96 long, narrow CsI scintillators, stacked in 8 layers, alternating in orientation so that the location and spread of the deposited energy can be determined. The plastic anticoincidence scintillator around the outside is made of 89 individual sections so that it can distinguish charged particles coming from the direction of the incident gamma ray and ignore others. Figs from [https://www-glast.stanford.edu]

Extensive catalogue of Gamma sources >4σ (no transients!) after 8 years of measurement [arxiv:1902.10045]:

5065	sources with 50 MeV > E> 1 TeV,
> 3130	associated with active galaxies of the blazar
239	Pulsars
75	extended sources (not point like)

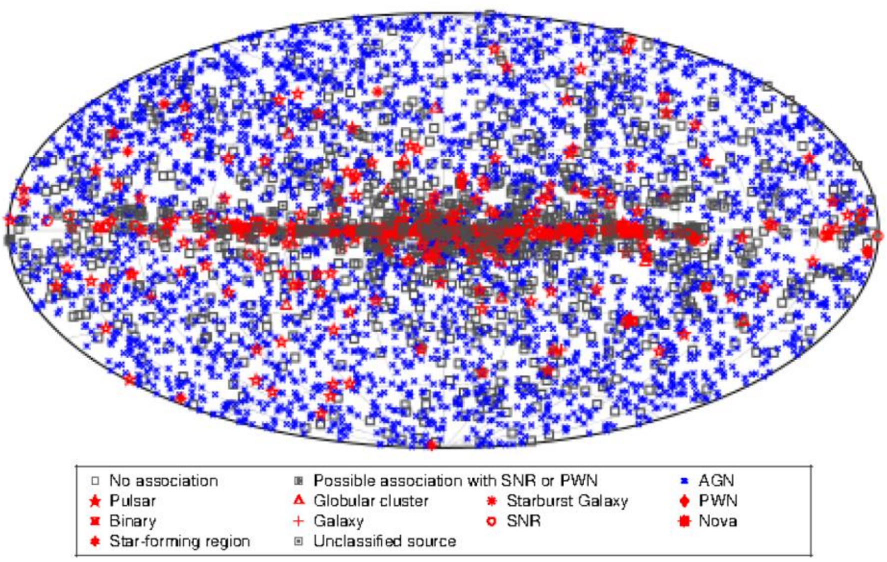

Full sky map showing sources by source class (see legend). Taken from [arxiv:1902.10045].

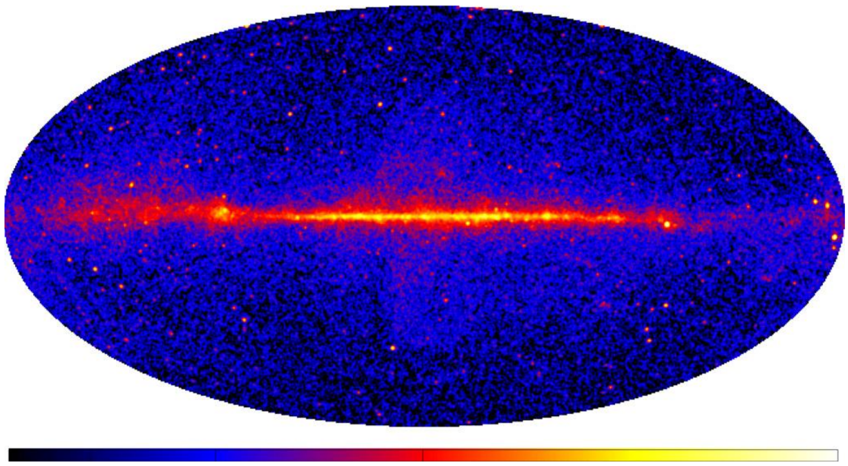

Sky map of γ -ray counts above 10 GeV in Galactic coordinates. The Galactic center is at the center of the map. The color code displays the flux of gamma rays aboe 10GeV per solid angle. Taken from [The Astrophys. J. Supp. Series, 209(2013)34.

Air Čerenkov Gamma Telescopes:

Čerenkov light of an air-shower illuminates area of ~10^5 m² on the ground with ~10-1000 ph./m² depending on the energy.

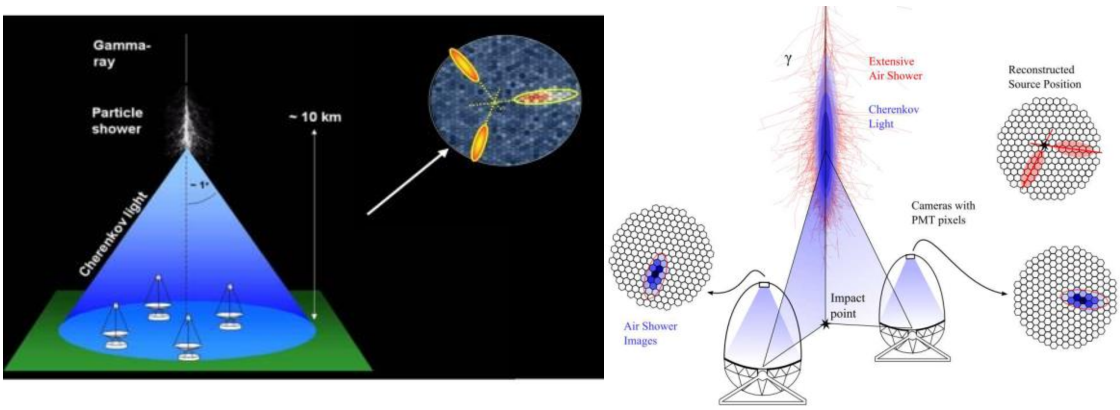

A large reflector placed on the ground can catch the Cherenkov light and focus it on a highly sensitive, fast integrated camera. With a single telescope the incoming particle direction is degenerate. The use of several telescopes breaks this degeneracy this as well as improve efficiently the reconstruction of several parameters of the shower (like the angular resolution), and the background rejection. Fig. from [http://isdc.unige.ch/cta/]

(Imaging Air shower Cherenkov Telescopes)

The light can be collected by large mirror telescopes an imaged on a very fast and sensitive camera.

The images can be used to reconstruct the energy, direction and type of primary particle.

HESS, MAGIC and VERITAS have led to boost in detection of extragalactic TeV sources. Many sources within galactic disc (HESS) detected

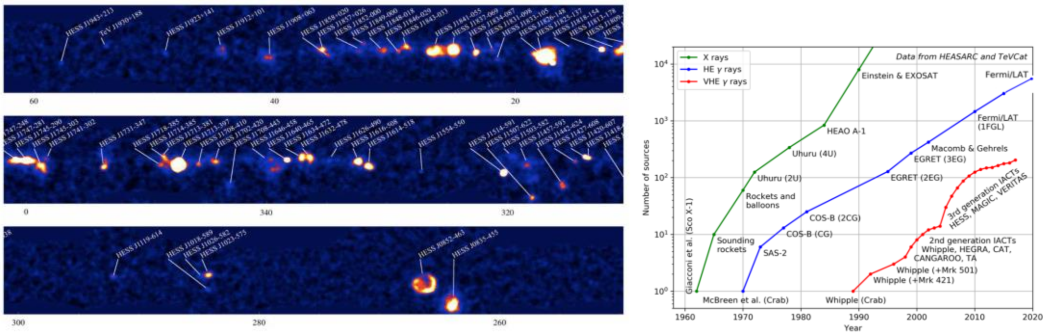

Left: H.E.S.S. Galactic Plane Survey, with source identifiers indicated. Fig from [https://www.mpi-hd.mpg.de/hfm/HESS/pages/home/som/2012/09/]. Right: Number of detected x-ray, gamma and TeV sources (adapted from https://raw.githubusercontent.com/sfegan/kifune-plot/master/kifune.png).

Main observations:

SN remnants:

- Detection of pulsed TeV emission of crab nebula

→ Cannot be from synchrotron radiation, as radius would be too large!

→ Inverse Compton Scattering!

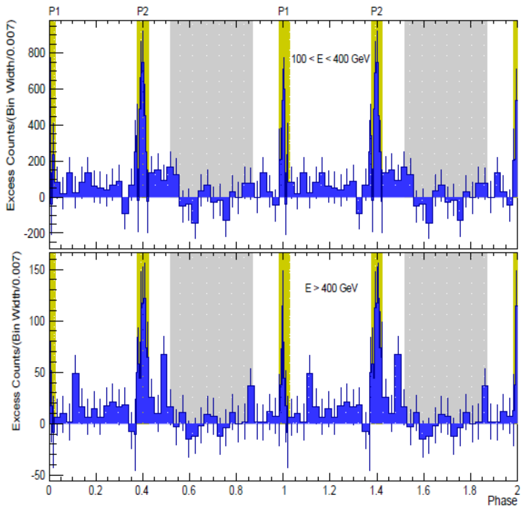

Pulse profile of the Crab pulsar between 100 and 400GeV (upper panel) and above 400 GeV (bottom panel). The pulse profile, shown twice for clarity, is background subtracted. The bin width around the two peaks is 4 times smaller (0.007) than the rest (0.027) in order to highlight the sharpness of the peaks. Yellow-dashed areas identify the phase intervals of the two peaks, whereas the gray areas show the offpulse region. Taken from [A&A, 585 (2016) A133]

- Energie spectrum with gammas up to 30 TeV ($3*10^{16}$eV)

→ No satisfactory model yet that can explain all observations (spectral shape,…)

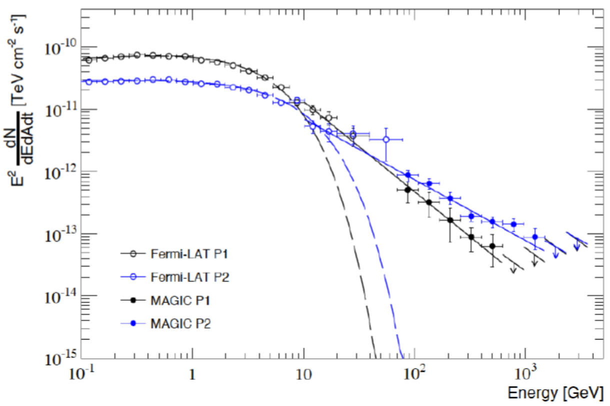

Combined FERMI-MAGIC measurement of Crab pulsar

MAGIC Fermi measurement of Crab pulsar: Inverse Compton effect

Blazars: Active Galactic Nuclei (AGN) with Jets pointed towards us:
Model: Influx of matter onto central massive black hole.
Flux variation very fast: MAGIC observation of IC310: $t_{var} \sim 10\ min$
→Small volume of source: $R_{var} = c \cdot t_{var} \sim 2 \cdot 10^{11}\ m$

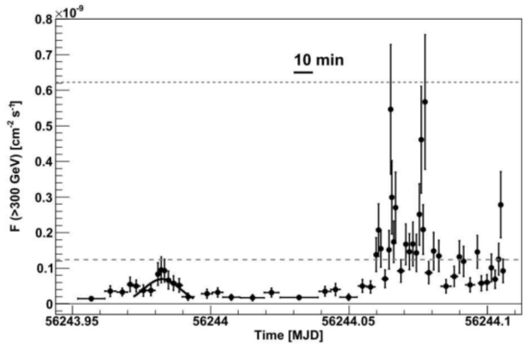

Left: High-energy gamma rays flux variation of IC 310 observed with the MAGIC telescopes in the night of November 12th to 13th, 2012. The emission doubled on the timescales of 5 min, much shorter than the size of the black hole (estimated to be 20min after taking into account shorter time variability of the jet due to relativistic effect), indicating that the gamma ray emissions occur in much smaller regions than the black hole. (Credit: The MAGIC Collaboration)

Compare to Schwarzschild radius of object with $2 \cdot 10^8 M_\odot$:

$$R_s = \frac{2MG}{c^2} \sim 1.5 \cdot 10^{11} m$$

→ Acceleration very close to the BH!

Search for correlation with arrival directions from Ice Cube Neutrino telescope:

The IceCube Collaboration *et al.*, *Science* **361**, 146 (2018)

RESEARCH ARTICLE SUMMARY

NEUTRINO ASTROPHYSICS

Multimessenger observations of a flaring blazar coincident with high-energy neutrino IceCube-170922A

The IceCube Collaboration, *Fermi*-LAT, MAGIC, *AGILE*, ASAS-SN, HAWC, H.E.S.S., *INTEGRAL*, Kanata, Kiso, Kapteyn, Liverpool Telescope, Subaru, *Swift/NuSTAR*, VERITAS, and VLA/17B-403 teams*†

Birth of neutrino multi-messenger astronomy:

22.Sept 2017: Observation of 290 TeV (2.9*10^{14}eV) Neutrino coincident in source position and time with flaring γ-ray blazar: FERMI LAT, MAGIC, … many thousand authors!

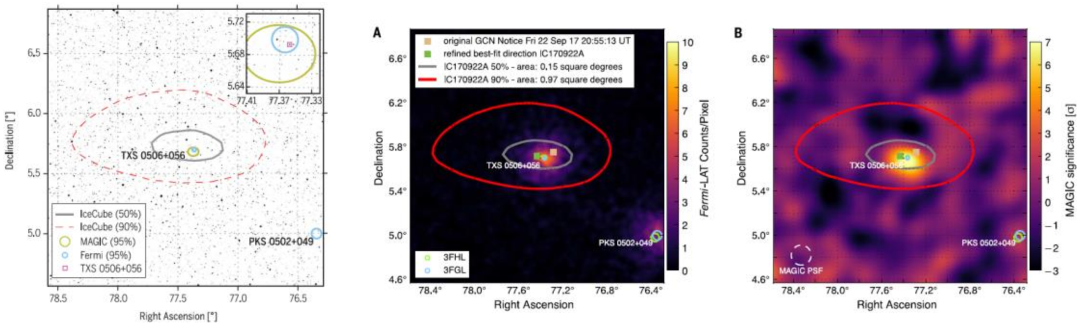

Sky position of IceCube-170922A in J2000 equatorial coordinates overlaying the g-ray counts from Fermi-LAT above 1 GeV (A) and the signal significance as observed by MAGIC (B) in this region.

Observation with ICECUBE was complemented by very high energy γ-ray observation with MAGIC on 28th of Sept.

- ➔ Blazars very promising candidate for acceleration to required energies!

Supernova explosions:

Supernovae of type II are triggered by gravitational collapse at the end of fusion process (no fuel available). Gravitational energy is transformed into an explosion. Only stars with mass to bring up sufficient gravitational energy can trigger a SN explosion: $M_C \sim 8\ M_\odot$.

Process leading to SN explosion for star with $M \sim 20\ M_\odot$:

Once hydrogen in the stellar core is depleted and is dominated by Helium: gravitational pressure will be higher than radiation power.

→Star contracts, Temperature increases, H-shell is pushed outward (can still undergo fusion in spherical shell)

→Fusion from helium to carbon and oxygen starts

→Once helium is depleted fusion rate reduces, gravitational pressure exceeds radiation pressure, temperature increases

→Fusion from carbon and oxygen to neon, manganese, silicon and sulphur starts

→In the last step Silicon is fused to iron

→Onion shell structure:

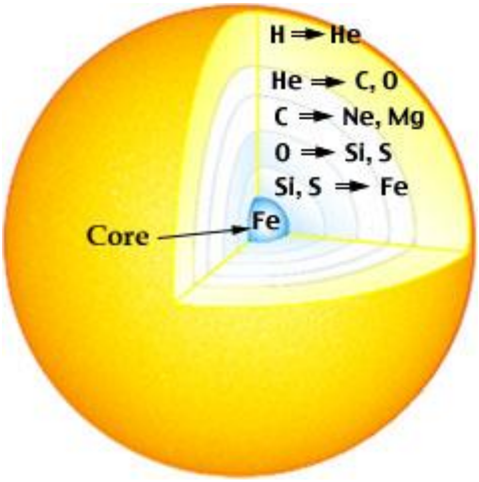

Durations of different burning cycles vary greatly:

Hydrogen	Helium	Carbon	Oxygen	Neon	Silicon
10^6	$5 \cdot 10^5$	600	0.5	1	0.004

For less massive stars evolution is similar, but constrained by the gravitational pressure and, hence, by the core temperature. If temperature is not high enough, next burning cycle cannot be ignited

In core collapse SN:

Once silicon is depleted:

→No further thermonuclear reactions

→No more radiation pressure to counteract gravitational pressure

→Gravitational collapse

→Core mass exceeds Chandrasekhar mass limit $M_{Cha} \sim 1.4 M_\odot$

→Core becomes instable and implodes

→Electrons are captured by protons: $p + e^- \rightarrow n + \nu_e$

→Emission of $\sim 10^{57}$neutrinos within $\sim 0.1s$!
→Transport of $\sim 10^{57} \cdot 10\ MeV = \ 10^{58} MeV$ in form of neutrinos away from core
→Compression of core to density $\rho \sim 2.5 \cdot 10^{14} g\ cm^{-3}$ and temperature $T \sim 10^{11} K$
→Collision of outer core onto central dense region
→Rebound shock wave with speed $v \sim \frac{1}{3} c$
→Rebound shock wave and neutrinos collide with outer shells of star and ignite explosion

	Core density	Core radius:
Core before implosion:	$\rho_i \sim 10^{11} g\ cm^{-3}$	$\sim 10^3 km$
Before reaching M_{Cha}		$\sim 10^2 km$
After collapse:	$\rho_{ii} \sim 2.5 \cdot 10^{14} g\ cm^{-3}$	$\sim 20\ km$